



Bifurcation Analysis of a Belousov–Zhabotinsky Reaction Model

Xiaoli Wang

*Department of Mathematics,
Beijing University of Chemical Technology,
15 Beisanhuan East Road, Chaoyang District,
Beijing 100029, P. R. China
759212592@qq.com*

Yu Chang*

*Department of Mathematics,
Beijing University of Chemical Technology,
15 Beisanhuan East Road, Chaoyang District,
Beijing 100029, P. R. China
changyu@mail.buct.edu.cn*

Dashun Xu

*Department of Mathematics,
Southern Illinois University, Carbondale,
IL 62901, USA
dashunxu@siu.edu*

Received January 15, 2015

We investigate the bifurcation phenomena in a Belousov–Zhabotinsky reaction model by applying Hopf bifurcation theory in frequency domain and harmonic balance method. The high accurate predictions, i.e. fourth-order harmonic balance approximation, on frequencies, amplitudes, and approximation expressions for periodic solutions emerging from Hopf bifurcation are provided. We also detect the stability and location of these periodic solutions. Numerical simulations not only confirm the theoretical analysis results but also illustrate some complex oscillations such as a cascade of period-doubling bifurcation, quasi-periodic solution, and period-doubling route to chaos. All these results improve the understanding of the dynamics of the model.

Keywords: Belousov–Zhabotinsky reaction; frequency domain; fourth-order harmonic balance.

1. Introduction

Belousov–Zhabotinsky (BZ) reaction is a family of chemical oscillation reaction, which is the oxidation and bromination of an organic compound

[Györgyi & Field, 1991]. It is well known for its rich and complex oscillations. A great deal of experimental and numerical simulation studies suggest that BZ reaction can exhibit various types of oscillations

*Author for correspondence

and complex dynamics, such as heterogeneous oscillation [Kuhnert, 1986], spiral waves [Keener & Tyson, 1986], period-doubling cascade [Györgyi & Field, 1991], deterministic chaos [Zhang *et al.*, 1993], chemical turbulence [Zhou & Yang, 2000], hyperchaos [Li *et al.*, 2002a], mesoscopic dynamical behavior [Li & Zhu, 2004], breathing front dynamics [Marts *et al.*, 2004], coexistence of two bifurcation regimes [Wang *et al.*, 2005], period-doubling and chaotic oscillations [Zong *et al.*, 2007], chaotic bursters [Bi, 2010]. In addition, Dolzmann *et al.* [2007] reported complex optical behavior in a nonstationary ferroin catalyzed BZ reaction. Guo *et al.* [2014] studied the dynamical behavior in the spatial-temporal domain for a BZ reaction by using a spatial-temporal domain identification and frequency domain analysis approach.

A large number of mathematical models have been developed to describe the BZ reaction in detail. The models proposed by Györgyi and Field [1991, 1992] have attracted a great deal of attention from researchers in different fields [Li *et al.*, 2002b; Zong *et al.*, 2007; Freire *et al.*, 2009; Li & Chang, 2012; Li, 2012]. In 1991, Györgyi *et al.* [1991] proposed a 11-variable BZ reaction model in a well-mixed, continuous-flow, stirred tank reactor (CSTR). Although this model can reproduce the behaviors experimentally observed at low CSTR flow rates, it is difficult to analyze the dynamical structure of the system. Then, the authors [Györgyi & Field, 1991] simplified the 11-variable model to a 7-variable model, and the 7-variable model was further reduced to two 4-variable models and one 3-variable model. Complex oscillations and chaotic dynamics in the 4-variable models are consistent with those experimentally observed at both high and low CSTR flow rates. Some studies of dynamical behaviors in one of 4-variable models, model D_{EQ} , have been reported. Györgyi and Field [1991] numerically showed complex oscillations in this model including periodic window, a cascade of period-doubling and chaos at low flow rates, complex limit cycles and chaos at high flow rates. Li *et al.* [2002b] studied chaos synchronization at low flow rate. Zong *et al.* [2007] experimentally and numerically investigated dynamical behaviors at high flow rate, and they found some complex oscillations such as mixed-mode oscillation

at low flow rate, periodic-doubling oscillation and chaos at high flow rate. Li and Chang [2012] theoretically analyzed Hopf bifurcation in time domain at both low and high flow rates. By applying Hopf bifurcation theory in frequency domain and second-order harmonic balance method, Li [2012] provided the estimates of frequencies and amplitudes, the explicit approximation expressions for the periodic oscillations emerging from Hopf bifurcation.

In this work, we further study the bifurcations in this 4-variable BZ reaction model D_{EQ} . By using Hopf bifurcation theorem in frequency domain [Mees & Chua, 1979; Moiola & Chen, 1996], we theoretically analyze Hopf bifurcation of the model. We provide higher accurate predictions on frequencies, amplitudes, and explicit formulas of periodic solutions arising from Hopf bifurcation by applying fourth-order harmonic balance method [Mees, 1981; Moiola *et al.*, 1991; Moiola & Chen, 1993, 1996]. The stability and location of these periodic solutions are also detected. In addition, we investigate the bifurcations of periodic orbit emerging from Hopf bifurcation. Furthermore, our numerical simulations show some new system behaviors including torus bifurcation at both low and high flow rates, period-doubling bifurcation, a cascade of period-doubling bifurcation and period-doubling route to chaos at high flow rate. All these results help to understand the dynamics of the BZ reaction.

The rest of article is organized as follows: In Sec. 2, we analyze the existence of Hopf bifurcation in frequency domain. In Sec. 3, the frequencies, amplitudes of periodic solutions generated from Hopf bifurcation and their explicit expressions are presented by fourth-order harmonic balance method. We also detect the stability and location of these periodic solutions. Numerical simulations are shown in Sec. 4 to verify the theoretical analysis results and display the complex dynamics. Section 5 contains the conclusions.

2. Equilibrium Points and Bifurcations

2.1. BZ reaction model

Consider the following BZ model.

$$\left\{ \begin{aligned}
 \frac{d[\text{Br}^-]}{dt} &= -k_{D1}[\text{H}^+][\text{Br}^-][\text{HBrO}_2] - k_{D2}[\text{BrO}_3^-][\text{H}^+]^2[\text{Br}^-] + k_{D7}[\text{Ce(IV)}][\text{BrMA}] \\
 &\quad + k_{D8}[\text{MA}]_{QSS}[\text{BrMA}] + k_f([\text{Br}^-]_{mf} - [\text{Br}^-]) \\
 \frac{d[\text{HBrO}_2]}{dt} &= -k_{D1}[\text{H}^+][\text{Br}^-][\text{HBrO}_2] + k_{D2}[\text{BrO}_3^-][\text{H}^+]^2[\text{Br}^-] - 2k_{D3}[\text{HBrO}_2]^2 \\
 &\quad + 0.5k_{D4}[\text{H}^+]([\text{Ce}]_{\text{tot}} - [\text{Ce(IV)}])[\text{BrO}_2]_{\text{EQ}} - 0.5k_{D5}[\text{HBrO}_2][\text{Ce(IV)}] \\
 &\quad + k_f([\text{HBrO}_2]_{mf} - [\text{HBrO}_2]) \\
 \frac{d[\text{Ce(IV)}]}{dt} &= k_{D4}[\text{H}^+]([\text{Ce}]_{\text{tot}} - [\text{Ce(IV)}])[\text{BrO}_2]_{\text{EQ}} - k_{D5}[\text{HBrO}_2][\text{Ce(IV)}] - k_{D6}[\text{MA}][\text{Ce(IV)}] \\
 &\quad - k_{D7}[\text{Ce(IV)}][\text{BrMA}] + k_f([\text{Ce(IV)}]_{mf} - [\text{Ce(IV)}]) \\
 \frac{d[\text{BrMA}]}{dt} &= 2k_{D1}[\text{H}^+][\text{Br}^-][\text{HBrO}_2] + k_{D2}[\text{BrO}_3^-][\text{H}^+]^2[\text{Br}^-] + k_{D3}[\text{HBrO}_2]^2 \\
 &\quad - k_{D7}[\text{Ce(IV)}][\text{BrMA}] - k_{D8}[\text{MA}]_{QSS} + k_f([\text{BrMA}]_{mf} - [\text{BrMA}]),
 \end{aligned} \right. \quad (1)$$

where



$$[\text{MA}]_{QSS} = -k_{C10}[\text{BrMA}] + \frac{\sqrt{(k_{C10}[\text{BrMA}])^2 + 8k_{C8}k_{C11}[\text{Ce(IV)}]}}{4k_{C11}},$$

$$[\text{BrO}_2]_{\text{EQ}} = \sqrt{\frac{k_{C4}[\text{HBrO}_2]}{k_{C5}}}, \quad [\text{Ce}]_{\text{tot}} = [\text{Ce(III)}]_{mf}.$$

$[\cdot]$ denotes the concentration of the component. $[\cdot]_{mf}$ refers to the mixed-feed concentration of the component, which is assumed to be zero for state variables [Györgyi & Field, 1991]. The four state variables in this model are the concentrations of bromide ion Br^- , bromous acid HBrO_2 , cerium ion Ce(IV) and bromalonic acid BrMA . H^+ and BrO_3^- are hydrogen ion and bromate ion, respectively. MA is malonic acid. The parameter k_f represents CSTR flow rate. The parameters k_{Di} ($i = 1, \dots, 8$) and k_{Cj} ($j = 4, 5, 8, 10, 11$) are constants, and their meanings can be found in [Györgyi & Field, 1991].

In this work, we further investigate bifurcations in BZ reaction model (1). The flow rate k_f is taken as bifurcation parameter, and other parameter values are chosen to be:

$$\begin{aligned}
 [\text{BrO}_3^-] &= 0.1 \text{ M}, & [\text{H}^+] &= 0.38 \text{ M}, \\
 [\text{MA}] &= 0.25 \text{ M}, & [\text{Ce(III)}] &= 8.33 \times 10^{-4} \text{ M},
 \end{aligned}$$

$$\begin{aligned}
 k_{D1} &= 2 \times 10^6 \text{ M}^{-2}\text{s}^{-1}, & k_{D2} &= 2.0 \text{ M}^{-3}\text{s}^{-1}, \\
 k_{D3} &= 3 \times 10^3 \text{ M}^{-1}\text{s}^{-1}, & k_{D4} &= 6.2 \times 10^4 \text{ M}^{-2}\text{s}^{-1}, \\
 k_{D5} &= 7 \times 10^3 \text{ M}^{-1}\text{s}^{-1}, & k_{D6} &= 0.3 \text{ M}^{-1}\text{s}^{-1}, \\
 k_{D7} &= 30 \text{ M}^{-1}\text{s}^{-1}, & k_{D8} &= 2.4 \times 10^4 \text{ M}^{-1}\text{s}^{-1}, \\
 k_{C4} &= 0.858 \text{ s}^{-1}, & k_{C5} &= 4.2 \times 10^7 \text{ M}^{-1}\text{s}^{-1}, \\
 k_{C8} &= 0.3 [\text{MA}]\text{s}^{-1}, & k_{C10} &= 2.4 \times 10^4 \text{ M}^{-1}\text{s}^{-1}, \\
 k_{C11} &= 3 \times 10^9 \text{ M}^{-1}\text{s}^{-1}.
 \end{aligned}$$

According to [Wiggins, 1990], simple qualitative analysis gives the following conclusion:

Conclusion 1

- For $2.0 \times 10^{-4} < k_f < 6.05172 \times 10^{-4}$ and $1.54738 \times 10^{-3} < k_f < 3.0 \times 10^{-2}$, system (1) has a stable node;

- For $6.05172 \times 10^{-4} < k_f < 1.54738 \times 10^{-3}$, system (1) has an unstable node;
- For $k_f^1 = 6.05172 \times 10^{-4}$ and $k_f^2 = 1.54738 \times 10^{-3}$, system (1) has two nonhyperbolic equilibrium points with a single pair of pure imaginary eigenvalues.

2.2. Hopf bifurcation for equilibrium point in frequency domain

In order to apply Hopf bifurcation theorem in frequency domain [Mees & Chua, 1979; Moiola &

Chen, 1996], model (1) is rewritten in the following form:

$$\dot{x} = A(k)x + Bg(y) \quad (2)$$

together with a second output equation

$$y = e = -Cx, \quad (3)$$

where

$$x = ([\text{Br}^-], [\text{HBrO}_2], [\text{Ce(IV)}], [\text{BrMA}])^T,$$

$$k = k_f, \quad e = (e_1, e_2, e_3, e_4)^T,$$

$$g(y) = (g_1, g_2, g_3, g_4)^T,$$

$$A(k) = \begin{pmatrix} -0.02888 - k & 0 & 0 & 0 \\ 0.02888 & -k & 0 & 0 \\ 0 & 0 & -0.075 - k & 0 \\ 0.02888 & 0 & 0 & -k \end{pmatrix}, \quad B = C = \begin{pmatrix} 1 & 0 & 0 & 0 \\ 0 & 1 & 0 & 0 \\ 0 & 0 & 1 & 0 \\ 0 & 0 & 0 & 1 \end{pmatrix},$$

$$g_1 = -7.6 \times 10^5 e_1 e_2 + 30 e_3 e_4 - 0.048 e_4^2 - 0.02 e_4 (5.76 e_4^2 - 18 e_3)^{0.5},$$

$$g_2 = -7.6 \times 10^5 e_1 e_2 - 6000 e_2^2 + 1.68369836 (0.000833 + e_3) (-e_2)^{0.5} - 3500 e_2 e_3,$$

$$g_3 = 3.36739672 (0.000833 + e_3) (-e_2)^{0.5} - 7000 e_2 e_3 - 30 e_3 e_4,$$

$$g_4 = 1.52 \times 10^6 e_1 e_2 + 3000 e_2^2 - 30 e_3 e_4 + 0.048 e_4^2 + 0.02 e_4 (5.76 e_4^2 - 18 e_3)^{0.5}.$$

Taking Laplace transforms on both sides of Eq. (2), we can separate Eq. (2) into a linear part with a transfer function

$$G(s; k) = C(sI - A(k))^{-1}B$$

$$= \begin{pmatrix} \frac{1}{0.02888 + k + s} & 0 & 0 & 0 \\ \frac{-0.002166 - 0.02888k - 0.02888s}{(k + s)(0.02888 + k + s)(0.075 + k + s)} & \frac{1}{k + s} & 0 & 0 \\ 0 & 0 & \frac{1}{0.075 + k + s} & 0 \\ \frac{0.02888}{(k + s)(0.02888 + k + s)} & 0 & 0 & \frac{1}{k + s} \end{pmatrix} \quad (4)$$

and a memoryless nonlinear part

$$u \triangleq g(e) \triangleq g(y). \quad (5)$$

It can be shown that systems (2) and (3) are equivalent to the feedback systems (4) and (5), where s is the Laplace variable, and the solution \hat{e} of $G(0; k)g(e) + e = 0$, i.e. the equilibrium point \hat{e} for systems (4) and (5), is equivalent to the equilibrium point \hat{x} in Eq. (2) [Mees & Chua, 1979].

Now we want to calculate the solution \hat{e} of the equation $G(0; k)g(e) + e = 0$ and investigate Hopf bifurcation in frequency domain at the equilibrium point \hat{e} for systems (4) and (5). Let $D_1 = \frac{\partial g}{\partial e}|_{\hat{e}}$, D_1 is the Jacobian matrix of the equilibrium point \hat{e} . The characteristic polynomial of transfer matrix $G(s; k)D_1$ is defined by

$$F(\lambda, s, k) = \det(\lambda I - G(s; k)D_1). \quad (6)$$

According to Hopf bifurcation theory in frequency domain [Mees & Chua, 1979; Moiola & Chen, 1996], Hopf bifurcation can occur at an equilibrium point \hat{e} for $k = k_0$ provided that two conditions are satisfied: (1) $F(\lambda, s, k) = 0$ has a single root $\hat{\lambda}(i\omega_0) = -1 + 0i$ when $k = k_0$, $s = i\omega_0$, where $i\omega_0$ is the pure imaginary eigenvalue of equilibrium point \hat{x} , equivalent to \hat{e} , of model (2) at $k = k_0$; (2) $\frac{\partial F(\lambda, i\omega, k)}{\partial \omega}|_{(-1, i\omega_0, k_0)}$ and $\frac{\partial F(\lambda, i\omega, k)}{\partial k}|_{(-1, i\omega_0, k_0)}$ are nonzero and not parallel.

Calculations show that systems (4) and (5) have two special equilibrium points:

- (a) $\hat{e}_1 = (-3.137488664 \times 10^{-6}, -3.914231394 \times 10^{-7}, -1.385673176 \times 10^{-5}, -1.539902738 \times 10^{-3})$ at $k_{01} = 6.05172 \times 10^{-4}$, with a single eigenvalue $\hat{\lambda}(i\omega_{01}) = -1 + 0i$, $\omega_{01} = 8.157976072 \times 10^{-2}$. $\frac{\partial F(\lambda, i\omega, k)}{\partial \omega}|_{(-1, i\omega_{01}, k_{01})} = 335.823 - 147.277i$, $\frac{\partial F(\lambda, i\omega, k)}{\partial k}|_{(-1, i\omega_{01}, k_{01})} \approx 69933.53854551 + 64276.656606i$.
- (b) $\hat{e}_2 = (-7.259249877 \times 10^{-7}, -3.711716701 \times 10^{-6}, -3.614864477 \times 10^{-5}, -1.34935985 \times 10^{-3})$ at $k_{02} = 1.54738 \times 10^{-3}$, with a single eigenvalue $\hat{\lambda}(i\omega_{02}) = -1 + 0i$, $\omega_{02} = 6.15181694412 \times 10^{-2}$. $\frac{\partial F(\lambda, i\omega, k)}{\partial \omega}|_{(-1, i\omega_{02}, k_{02})} = 975.955 - 250.035i$, $\frac{\partial F(\lambda, i\omega, k)}{\partial k}|_{(-1, i\omega_{02}, k_{02})} \approx -154714.716 - 181187.354i$.

Therefore, we have the following result:

Conclusion 2. For feedback systems (4) and (5), two Hopf bifurcations HB¹ and HB² can occur at two equilibrium points \hat{e}_1 for $k_{01} = 6.05172 \times 10^{-4}$ and \hat{e}_2 for $k_{02} = 1.54738 \times 10^{-3}$, respectively.

3. The Approximate Analysis and Stability of Periodic Orbits

3.1. Computations of frequency, amplitude and approximate analytical expression for periodic solution

In this section, by fourth-order harmonic balance method we wish to obtain a high accurate approximation of the periodic solution generated from Hopf bifurcation at equilibrium point \hat{e} . The fourth-order harmonic balance explicit formula [Mees, 1981; Moiola *et al.*, 1991; Moiola & Chen, 1993, 1996] is given by

$$e(t) \approx \hat{e} + \text{Re} \left(\sum_{n=0}^4 E^n \exp(in\hat{\omega}t) \right), \quad (7)$$

where $E^0 = V_{02}\hat{\theta}^2 + V_{04}\hat{\theta}^4$, $E^1 = V_{11}\hat{\theta} + V_{13}\hat{\theta}^3 + V_{15}\hat{\theta}^5$, $E^2 = V_{22}\hat{\theta}^2 + V_{24}\hat{\theta}^4$, $E^3 = V_{33}\hat{\theta}^3 + V_{35}\hat{\theta}^5$, $E^4 = V_{44}\hat{\theta}^4$. $\hat{\omega}$ and $\hat{\theta}$ denote the frequency and amplitude of periodic solution $e(t)$, respectively, both of which are the solutions of the following equation:

$$\hat{\lambda}(i\omega) = -1 - \theta^2 Z_1(\omega) - \theta^4 Z_2(\omega). \quad (8)$$

The explicit expressions of V_{ij} , $Z_1(\omega)$ and $Z_2(\omega)$ can be found in [Mees, 1981; Moiola *et al.*, 1991; Moiola & Chen, 1993, 1996].

In order to compute $\hat{\omega}$ and $\hat{\theta}$ for Eq. (8), we separate the real and imaginary parts of Eq. (8) as follows:

$$\begin{cases} \text{Re}[\hat{\lambda}(i\omega)] = -1 - \theta^2 \text{Re}[Z_1(\omega)] - \theta^4 \text{Re}[Z_2(\omega)] \\ \text{Im}[\hat{\lambda}(i\omega)] = -\theta^2 \text{Im}[Z_1(\omega)] - \theta^4 \text{Im}[Z_2(\omega)]. \end{cases} \quad (9)$$

Suppose $Z_2(\omega) \neq 0$. By eliminating θ^4 from (9), we obtain

$$\begin{aligned} \text{Re}[\hat{\lambda}(i\omega) + 1] \text{Im}[Z_2(\omega)] - \text{Re}[Z_2(\omega)] \text{Im}[\hat{\lambda}(i\omega)] \\ = (\text{Re}[Z_2(\omega)] \text{Im}[Z_1(\omega)] \\ - \text{Re}[Z_1(\omega)] \text{Im}[Z_2(\omega)]) \theta^2. \end{aligned} \quad (10)$$

We consider two cases.

Case I. $\text{Re}[Z_2(\omega)] \text{Im}[Z_1(\omega)] - \text{Re}[Z_1(\omega)] \text{Im}[Z_2(\omega)] \neq 0$. In this case, (10) can be rewritten as

$$\begin{aligned} \theta^2 = \frac{\text{Re}[\hat{\lambda}(i\omega) + 1] \text{Im}[Z_2(\omega)] - \text{Re}[Z_2(\omega)] \text{Im}[\hat{\lambda}(i\omega)]}{\text{Re}[Z_2(\omega)] \text{Im}[Z_1(\omega)] - \text{Re}[Z_1(\omega)] \text{Im}[Z_2(\omega)]} \\ \triangleq h(\omega). \end{aligned} \quad (11)$$

Substituting (11) into the Eq. (9) yields

$$\begin{aligned} \text{Re}[\hat{\lambda}(i\omega)] = -1 - h(\omega) \text{Re}[Z_1(\omega)] \\ - h^2(\omega) \text{Re}[Z_2(\omega)] \end{aligned} \quad (12)$$

for $\text{Re}[Z_2(\omega)] \neq 0$, and

$$\begin{aligned} \text{Im}[\hat{\lambda}(i\omega)] = -h(\omega) \text{Im}[Z_1(\omega)] \\ - h^2(\omega) \text{Im}[Z_2(\omega)] \end{aligned} \quad (13)$$

for $\text{Im}[Z_2(\omega)] \neq 0$.

In order to find the roots $\hat{\omega}$ of Eq. (12) or Eq. (13), we firstly choose a k in the left small neighborhood of Hopf bifurcation parameter k_0 , and

substitute k into Eq. (12) or Eq. (13) to obtain numerical values of $\hat{\omega}$ sufficiently close to ω_0 . Then by substituting $\hat{\omega}$ into (11), the value of $\hat{\theta}^2$ will be computed. If the value of $\hat{\theta}^2$ is positive, the periodic solution emerging from Hopf bifurcation appears for $k < k_0$. If the value of $\hat{\theta}^2$ is negative, then the bifurcated periodic solution appears not for $k < k_0$ but for $k > k_0$. We need to choose a k in the right small neighborhood of Hopf bifurcation parameter k_0 and compute $(\hat{\omega}, \hat{\theta})$.

Case II. $\text{Re}[Z_2(\omega)]\text{Im}[Z_1(\omega)] - \text{Re}[Z_1(\omega)]\text{Im}[Z_2(\omega)] = 0$. In this case, (10) becomes

$$\begin{aligned} & \text{Re}[\hat{\lambda}(i\omega) + 1]\text{Im}[Z_2(\omega)] \\ & - \text{Re}[Z_2(\omega)]\text{Im}[\hat{\lambda}(i\omega)] = 0. \end{aligned} \quad (14)$$

Similarly, we numerically compute the values of $\hat{\omega}$ sufficiently close to ω_0 from (14), and substitute $\hat{\omega}$ into (9) to obtain $\hat{\theta}^2$.

Following the procedure described above, we get the following results:

(I) The periodic orbit generated from HB¹ at \hat{e}_1 appears in the right neighborhood of $k_{01} = 6.05172 \times 10^{-4}$. For $k = 6.1045 \times 10^{-4}$, the fourth-order harmonic balance approximation expression of the periodic orbit with frequency

$$\hat{\omega} = 8.1068731623462 \times 10^{-2}$$

and amplitude

$$\hat{\theta} = 1.298375930657188 \times 10^{-7}$$

is given by

$$e(t) \approx \hat{e} + \text{Re} \left(\sum_{n=0}^4 E^n \exp(in\hat{\omega}t) \right),$$

where $\hat{e} = (-3.1072073515 \times 10^{-6}, -3.9738278184 \times 10^{-7}, -0.00001397138896, -0.00153491273)^T$,

$$\begin{aligned} E^0 &= 10^{-7} \times \begin{pmatrix} -0.001378244627313 \\ -0.000267374533455 \\ -0.000818866958143 \\ -0.218787694528839 \end{pmatrix}, \\ E^1 &= 10^{-7} \times \begin{pmatrix} -0.282277843257427 - 0.199006203039458i \\ 0.058826546219293 + 0.037503694716739i \\ 0.969152084883089 + 0.000000984037526i \\ 0.639531114456919 - 0.461923055003505i \end{pmatrix}, \\ E^2 &= 10^{-9} \times \begin{pmatrix} 0.151425449725114 - 0.134552850389603i \\ -0.052796538323410 - 0.018180057061660i \\ -0.302503844697538 + 0.339219531738535i \\ -0.146133743356638 + 0.408191526168601i \end{pmatrix}, \\ E^3 &= 10^{-11} \times \begin{pmatrix} 0.039716335296817 + 0.139511251979552i \\ 0.047818266031950 - 0.009187271976616i \\ -0.048469075034954 - 0.275277050341810i \\ -0.164469984571708 - 0.259894462511374i \end{pmatrix}, \\ E^4 &= 10^{-13} \times \begin{pmatrix} -0.116036542786798 - 0.032146459214479i \\ -0.029448309005695 + 0.034077496390071i \\ 0.181657291018815 + 0.091919330614548i \\ 0.250753242362002 + 0.019605241552955i \end{pmatrix}. \end{aligned}$$

(II) The periodic orbit generated from HB² at \hat{e}_2 appears in the left neighborhood of $k_{02} = 1.54738 \times 10^{-3}$. For $k = 1.547 \times 10^{-3}$, the fourth-order harmonic balance approximation expression of the periodic orbit

with frequency $\hat{\omega} = 6.1371869 \times 10^{-2}$ and amplitude $\hat{\theta} = 1.127697655889159 \times 10^{-6}$ is given by

$$e(t) \approx \hat{e} + \operatorname{Re} \left(\sum_{n=0}^4 E^n \exp(in\hat{\omega}t) \right),$$

where $\hat{e} = (-7.26348434 \times 10^{-7}, -3.708952782 \times 10^{-6}, -0.00003613998, -0.00134943716)^T$,

$$E^0 = 10^{-6} \times \begin{pmatrix} -0.000623603956585 \\ -0.003928409225123 \\ 0.004153785205925 \\ 0.444029053851815 \end{pmatrix},$$

$$E^1 = 10^{-6} \times \begin{pmatrix} -0.038670750332176 - 0.020612062812239i \\ 0.269759145025610 + 0.109490671930614i \\ 0.799757783398478 + 0.000144129922089i \\ 0.128949958701153 - 0.727175272445702i \end{pmatrix},$$

$$E^2 = 10^{-7} \times \begin{pmatrix} -0.018002678558810 + 0.008824105162330i \\ 0.040899606399917 - 0.136421339899872i \\ 0.021481701046379 - 0.307395359346716i \\ -0.122390983923579 - 0.032706421985678i \end{pmatrix},$$

$$E^3 = 10^{-8} \times \begin{pmatrix} -0.001459501068126 + 0.010447327621118i \\ -0.071257562757574 - 0.022986523108462i \\ -0.135523854145855 - 0.028414153561823i \\ -0.004915850436747 + 0.028006415605450i \end{pmatrix},$$

$$E^4 = 10^{-10} \times \begin{pmatrix} 0.046813279851679 + 0.037848638504768i \\ -0.156941803039144 + 0.382332592054964i \\ -0.236055807499592 + 0.635558102926264i \\ 0.086682305040796 - 0.035042300457125i \end{pmatrix}.$$

Periodic orbits calculated from our formulas (black curve) and by numerically solving differential equations (green “+”) are highly consistent with each other. Their graphs are shown in Figs. 1(a) and 1(b).

3.2. Detection of stability for periodic orbits

In [Jing *et al.*, 2002], it was shown that the periodic orbit bifurcated from Hopf bifurcation is stable if one of Conditions (I) and (II) is satisfied: Condition (I). The argument of $\hat{\lambda}(i\omega)$, $\arg(\hat{\lambda}(i\omega))$, decreases as ω increases in the neighborhood of $(\hat{\omega}, \hat{\theta})$, and $\arg(\frac{d\hat{\lambda}(i\omega)}{d\omega}/\frac{dL_2}{d(\theta^2)})|_{(\hat{\omega}, \hat{\theta})} < 0$; Condition (II). The argument of $\hat{\lambda}(i\omega)$, $\arg(\hat{\lambda}(i\omega))$, increases as ω

increases in the neighborhood of $(\hat{\omega}, \hat{\theta})$, and $\arg(\frac{d\hat{\lambda}(i\omega)}{d\omega}/\frac{dL_2}{d(\theta^2)})|_{(\hat{\omega}, \hat{\theta})} > 0$. Here, $L_2 = -1 - \theta^2 Z_1 \times (\omega) - \theta^4 Z_2(\omega)$. $(\hat{\omega}, \hat{\theta})$ is the frequency and amplitude of the periodic solution. $\frac{d\hat{\lambda}(i\omega)}{d\omega}$ is the tangent vector of $\hat{\lambda}(i\omega)$ along the increasing direction of ω , and $\frac{dL_2}{d(\theta^2)}$ denotes the tangent vector of L_2 along the increasing direction of θ^2 .

Note that

$$\frac{d\hat{\lambda}(i\omega)}{d\omega} \Big|_{(\hat{\omega}, \hat{\theta})} \approx \frac{\hat{\lambda}(i\hat{\omega}_1) - \hat{\lambda}(i\hat{\omega}_2)}{\hat{\omega}_1 - \hat{\omega}_2},$$

$$\frac{dL_2}{d(\theta^2)} \Big|_{(\hat{\omega}, \hat{\theta})} \approx -Z_1(\hat{\omega}) - 2\hat{\theta}^2 Z_2(\hat{\omega}),$$

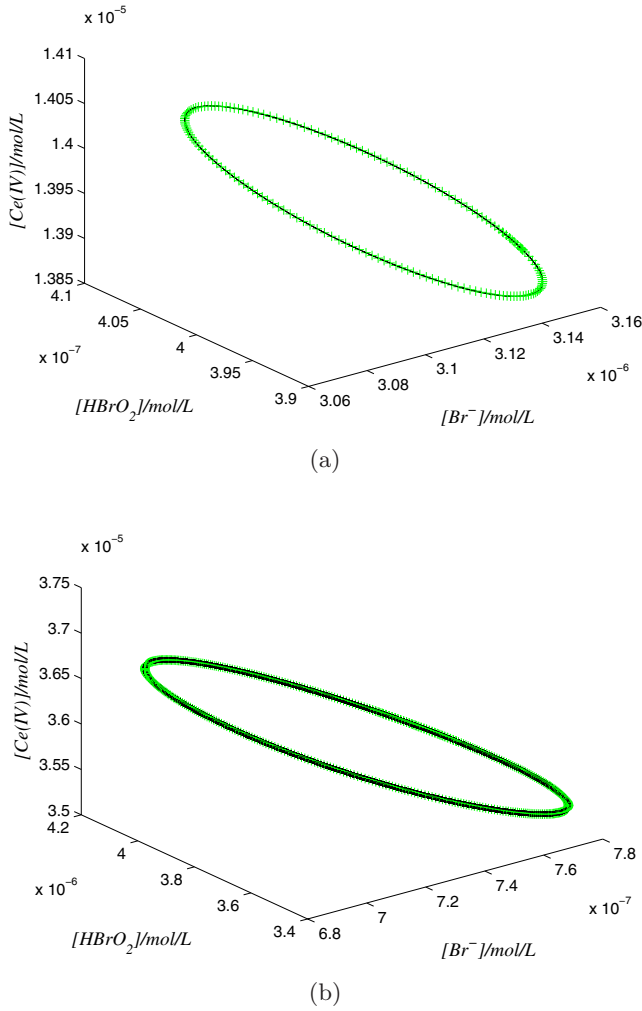


Fig. 1. The projections of periodic solutions (a) $k = 6.1045 \times 10^{-4}$ and (b) $k = 1.547 \times 10^{-3}$.

where both $\hat{\omega}_1$ and $\hat{\omega}_2$ are in the small neighborhood of $\hat{\omega}$ and sufficiently close to each other, thus we can determine the stability of periodic orbit by calculating $\frac{\hat{\lambda}(i\hat{\omega}_1) - \hat{\lambda}(i\hat{\omega}_2)}{\hat{\omega}_1 - \hat{\omega}_2}$ and $-Z_1(\hat{\omega}) - 2\hat{\theta}^2 Z_2(\hat{\omega})$.

For the periodic orbit with frequency $\hat{\omega} = 8.1068731623462 \times 10^{-2}$ at $k = 6.1045 \times 10^{-4}$, we choose $\hat{\omega}_1 = 8.1068731623462 \times 10^{-2}$ and $\hat{\omega}_2 = 8.10687317 \times 10^{-2}$, and have $\arg(\hat{\lambda}(i\hat{\omega}_1)) - \arg(\hat{\lambda}(i\hat{\omega}_2)) = 3.48684636719554 \times 10^{-10} > 0$,

$$\arg \left(\frac{d\hat{\lambda}(i\omega)}{\frac{d\omega}{dL_2}} \right) \bigg|_{(\hat{\omega}, \hat{\theta})} \approx \arg \left(\frac{\hat{\lambda}(i\hat{\omega}_1) - \hat{\lambda}(i\hat{\omega}_2)}{-Z_1(\hat{\omega}) - 2\hat{\theta}^2 Z_2(\hat{\omega})} \right) = -2.255624500755766 < 0.$$

Therefore, the periodic orbit bifurcated from HB¹ at $k = 6.1045 \times 10^{-4}$ is stable.

Similarly, for the periodic orbit with frequency $\hat{\omega} = 6.1371869 \times 10^{-2}$, by choosing

$$\hat{\omega}_1 = 6.1371869 \times 10^{-2} \quad \text{and}$$

$$\hat{\omega}_2 = 6.1371870 \times 10^{-2},$$

we compute

$$\arg(\hat{\lambda}(i\hat{\omega}_1)) - \arg(\hat{\lambda}(i\hat{\omega}_2)) = 1.680128924874680 \times 10^{-9} > 0$$

and

$$\arg \left(\frac{d\hat{\lambda}(i\omega)}{\frac{d\omega}{dL_2}} \right) \bigg|_{(\hat{\omega}, \hat{\theta})} \approx \arg \left(\frac{\frac{\hat{\lambda}(i\hat{\omega}_1) - \hat{\lambda}(i\hat{\omega}_2)}{\hat{\omega}_1 - \hat{\omega}_2}}{-Z_1(\hat{\omega}) - 2\hat{\theta}^2 Z_2(\hat{\omega})} \right) = -2.039280080314195 < 0.$$

Hence, the periodic orbit bifurcated from HB² at $k = 1.547 \times 10^{-3}$ is stable.

4. Numerical Simulations

In this section, we present numerical simulations to show bifurcations of periodic solutions, which emerge from Hopf bifurcation, and complex oscillations.

For convenience, we use the abbreviations: HB (Hopf bifurcation); PDB (period-doubling bifurcation); TR (torus bifurcation).

The bifurcation diagram of k_f versus $\text{MAX} \times [\text{Ce(IV)}]$ is given in Fig. 2 by using AUTO2007

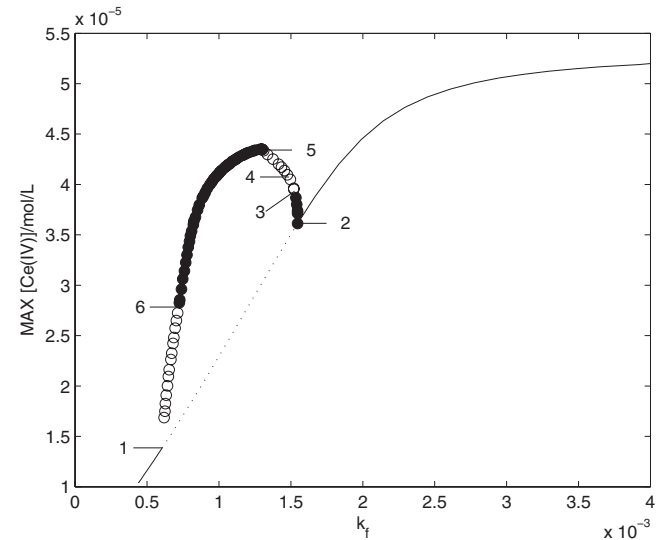


Fig. 2. The bifurcation diagram.

Table 1. Bifurcation points and k_f values in Fig. 2.

	HB ¹	HB ²	TR ³	PDB ⁴	PDB ⁵	TR ⁶
k_f	6.05172×10^{-4}	1.54738×10^{-3}	1.52493×10^{-3}	1.49535×10^{-3}	1.30792×10^{-3}	7.18684×10^{-4}

Table 2. The movement of Floquet multipliers.

λ_1	λ_2	λ_3	λ_4	k_f
1	$0.609334 + 0.707861i$	$0.609334 - 0.707861i$	7.75969×10^{-6}	
1	$0.526870 + 0.836141i$	$0.526870 - 0.836141i$	1.21215×10^{-5}	
1	$0.473870 + 0.898851i$	$0.473870 - 0.898851i$	3.95886×10^{-6}	TR ³
1	$-1.26165 + 0.762219i$	$-1.26165 - 0.762219i$	1.70197×10^{-6}	
1	-1.37868	-1.66829	1.53633×10^{-6}	
1	-0.89026	-2.73651	1.46015×10^{-6}	PDB ⁴
1	-0.729487	-3.53699	1.37755×10^{-6}	
1	-0.3647	-10.5471	5.87986×10^{-7}	
1	-0.217364	-30.6145	3.89576×10^{-7}	
1	-0.280294	-1.26862	-5.35722×10^{-6}	
1	-0.338771	-0.86487	-6.17477×10^{-6}	PDB ⁵
1	$0.364276 + 0.319971i$	$0.364276 - 0.319971i$	-4.31995×10^{-6}	
1	$0.596511 + 0.678982i$	$0.596511 - 0.678982i$	-3.32642×10^{-6}	
1	$0.733855 + 0.663588i$	$0.733855 - 0.663588i$	-8.32086×10^{-6}	
1	$0.755596 + 0.656842i$	$0.755596 - 0.656842i$	-8.92905×10^{-6}	TR ⁶
1	$0.777703 + 0.648871i$	$0.777703 - 0.648871i$	-9.59059×10^{-6}	
1	$0.821894 + 0.629984i$	$0.821894 - 0.629984i$	-1.18734×10^{-5}	

[Doedel *et al.*, 2007]. There are six types of bifurcations, which are listed in Table 1. The solid and dashed curves represent the stable and unstable equilibrium points, respectively. From Fig. 2, we can observe that the equilibrium point undergoes two bifurcations labeled as HB¹ and HB². The equilibrium point is stable for $k_f < k_f^1 = 6.05172 \times 10^{-4}$. At k_f^1 , a supercritical Hopf bifurcation HB¹ occurs, so that this equilibrium point loses its stability and a stable periodic orbit emerges from HB¹. With a further increase in k_f , the equilibrium point gains stability back through supercritical HB² at $k_f^2 = 1.54738 \times 10^{-3}$ until $k_f = 3.0 \times 10^{-2}$.

Figure 2 also shows the branch of the periodic solution generated from HB². The filled and open circles indicate the stable and unstable periodic solutions, respectively. Table 2 shows the movement of Floquet multipliers along the branch of periodic orbit between $k_f = 7.13906 \times 10^{-4}$ and $k_f = 1.53081 \times 10^{-3}$. A stable periodic solution emerges from HB² at $k_f = 1.54643 \times 10^{-3}$ due to supercritical Hopf bifurcation HB², the corresponding four Floquet multipliers are $\{1, 0.914603, 0.613985, 0.0000219968\}$. As k_f decreases, a pair of complex conjugate multipliers $0.526870 \pm 0.836141i$ cross

the unit circle from the inside to the outside unit circle, so that a torus bifurcation TR³ occurs at $k_f^3 = 1.52493 \times 10^{-3}$, and the periodic solution loses its stability. At $k_f = 1.5248 \times 10^{-3}$, i.e. at high flow rate, we find a chaotic orbit with Lyapunov exponents $\{0.0028469, 0, -0.00068817, -3.3209\}$, which is shown in Fig. 3.

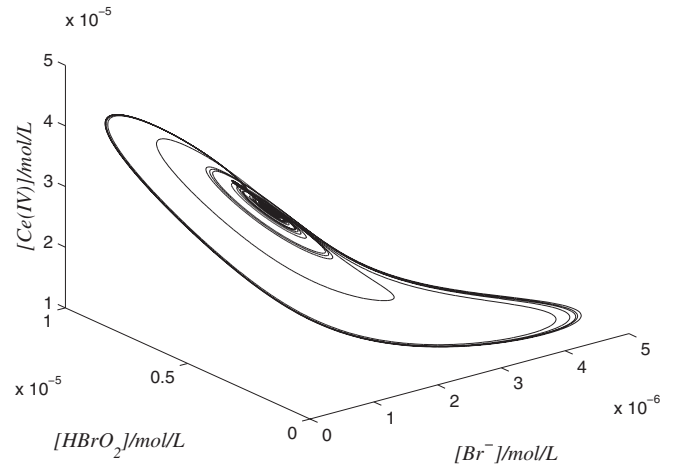
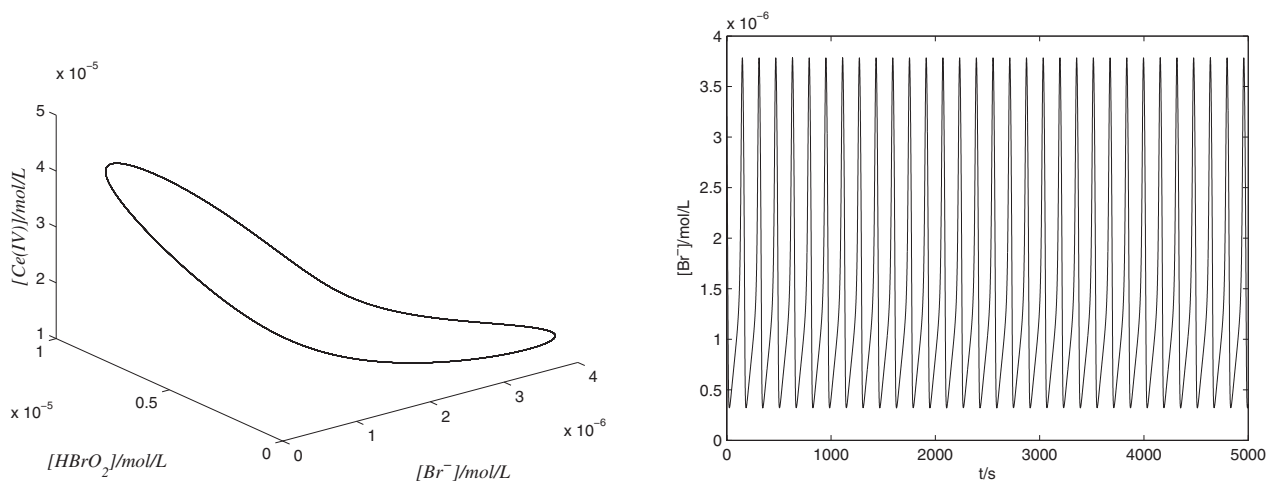
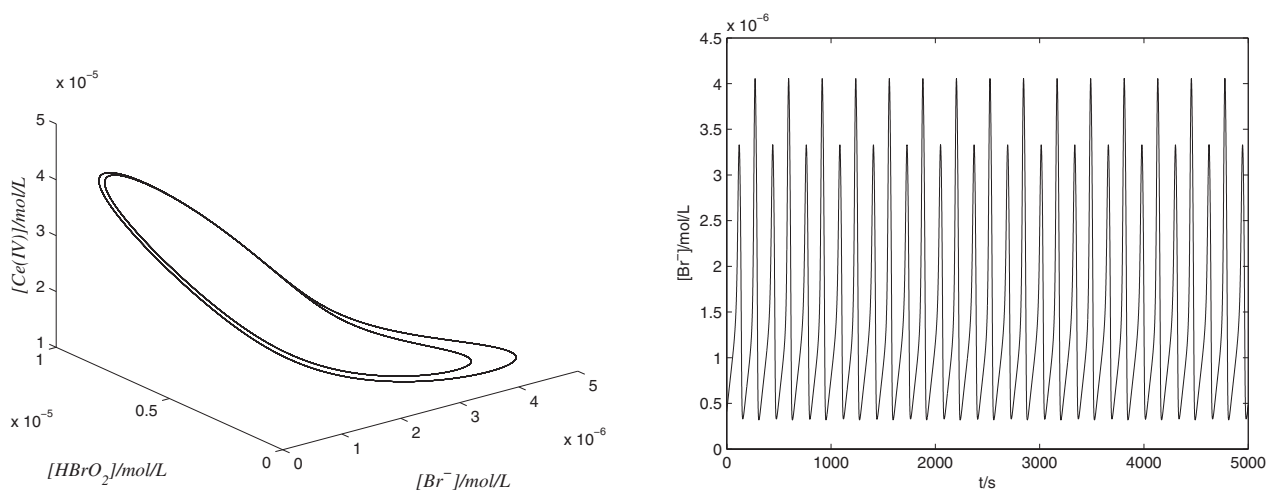


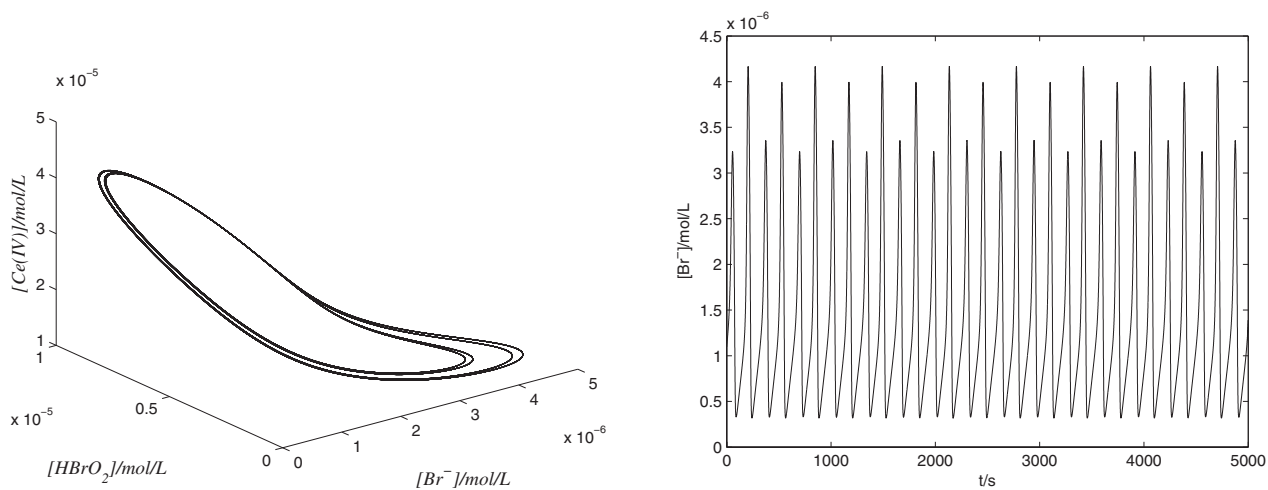
Fig. 3. The projection of a chaotic trajectory for $k_f = 1.5248 \times 10^{-3}$.



(a) Period-one orbit for $k_f = 1.3075 \times 10^{-3}$.

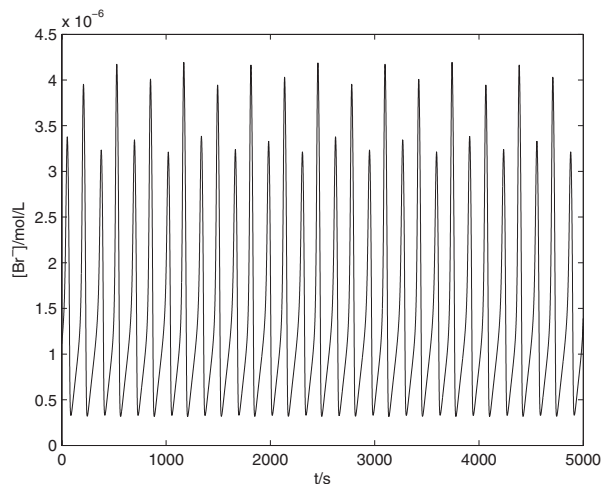
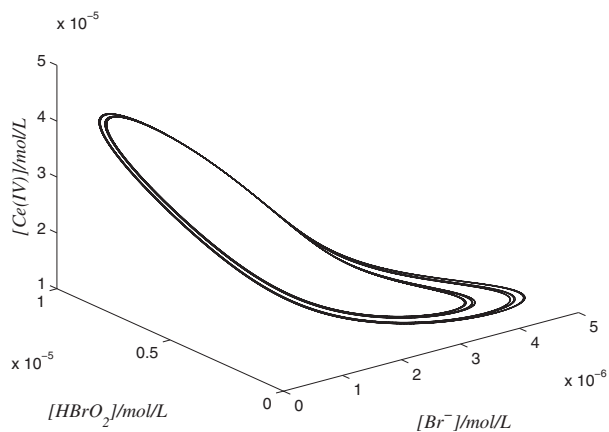


(b) Period-two orbit for $k_f = 1.3085 \times 10^{-3}$.

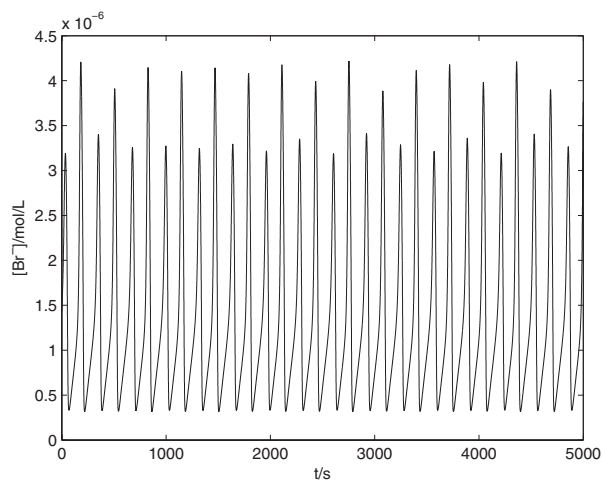
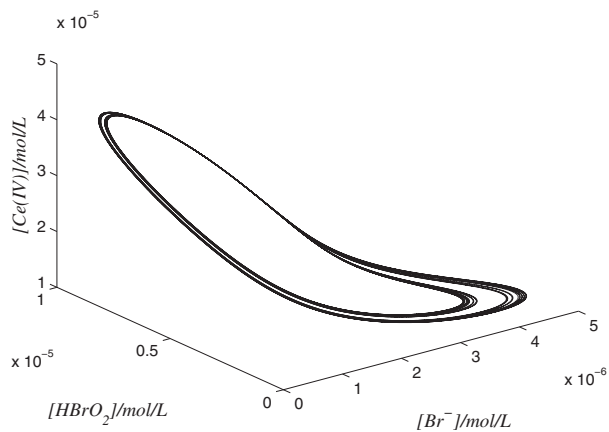


(c) Period-four orbit for $k_f = 1.3086 \times 10^{-3}$.

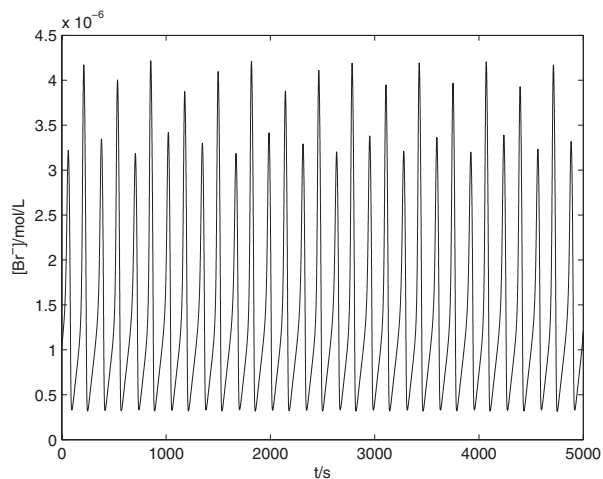
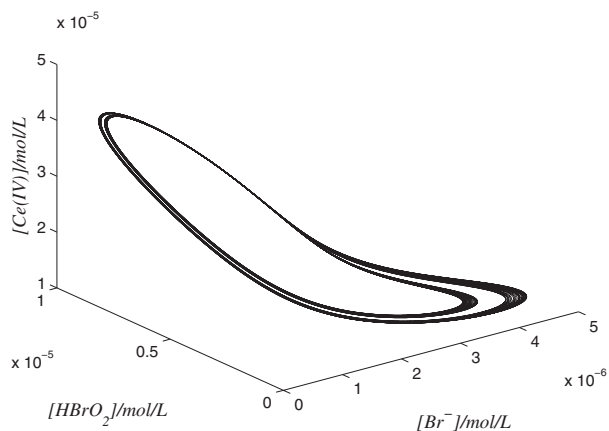
Fig. 4. The numerical simulations of period-doubling cascade to chaos.



(d) Period-eight orbit for $k_f = 1.30862 \times 10^{-3}$.



(e) Period-16 orbit for $k_f = 1.30864 \times 10^{-3}$.



(f) A chaotic orbit for $k_f = 1.308640802 \times 10^{-3}$.

Fig. 4. (Continued)

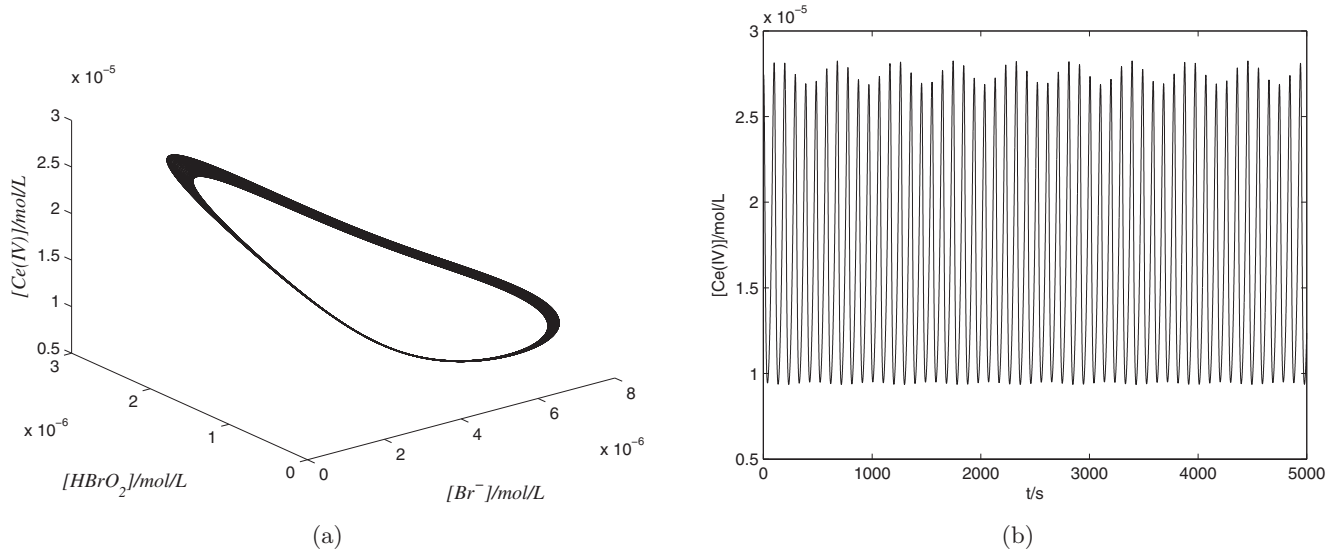


Fig. 5. The projection of a quasi-periodic trajectory and its time series for $k_f = 7.156 \times 10^{-4}$.

With a further decrease in k_f , one of the multipliers passes across the unit circle at -1 for $k_f^4 = 1.49535 \times 10^{-3}$, which results in the period-doubling bifurcation PDB⁴, and the unstable periodic solution has not regained its stability until PDB⁵ at $k_f^5 = 1.30792 \times 10^{-3}$. When k_f is slightly greater than k_f^5 , the periodic solution undergoes a cascade of period-doubling bifurcation. Figures 4(a)–4(e) show the stable period-one orbit for $k_f = 1.3075 \times 10^{-3}$, period-two orbit for $k_f = 1.3085 \times 10^{-3}$, period-four orbit for $k_f = 1.3086 \times 10^{-3}$, period-eight orbit for $k_f = 1.30862 \times 10^{-3}$ and period-16 orbit for $k_f = 1.30864 \times 10^{-3}$, respectively. A chaotic orbit resulted from this cascade is presented in Fig. 4(f). Chaotic oscillation is observed in the region around $k_f \in [1.308640802 \times 10^{-3}, 1.52492 \times 10^{-3}]$. When k_f continuously decreases from $k_f^5 = 1.30792 \times 10^{-3}$ and reaches $k_f^6 = 7.18684 \times 10^{-4}$, a pair of complex conjugate multipliers $0.733855 \pm 0.663588i$ pass across the unit circle from the inside to the outside unit circle, so that the periodic solution encounters the torus bifurcation TR⁶ and loses its stability. Thus, a quasi-periodic orbit arises from this bifurcation. Figure 5 shows the projection of a quasi-periodic solution at $k_f = 7.156 \times 10^{-4}$. When $k_f = 7.1 \times 10^{-4}$, i.e. at low flow rate, we also find a chaotic attractor with Lyapunov exponents $\{0.004073, 0, -0.00064437, -2.2323\}$, which is presented in Fig. 6. Numerical simulations in Figs. 1–6 suggest that the flow rate k_f has important effects on bifurcations and dynamics of BZ reaction model.

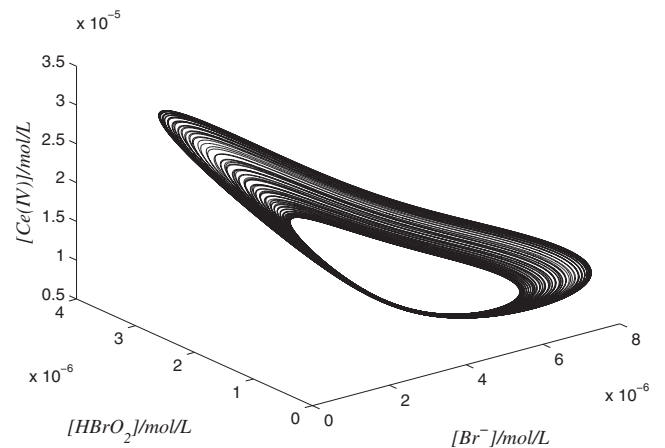


Fig. 6. The projection of a chaotic trajectory for $k_f = 7.1 \times 10^{-4}$.

5. Conclusion

Bifurcations of the BZ reaction model have been carefully and rigorously studied. Fourth-order harmonic balance method allowed us to obtain higher accurate predictions on frequencies and amplitudes for periodic solutions emerging from Hopf bifurcation. The explicit approximation expressions of the periodic solutions are also presented. Numerical simulations show several dynamical bifurcations emerging from Hopf bifurcation, including period-doubling bifurcation, chaotic attractor resulting from a cascade of period-doubling bifurcation, and torus bifurcation. We can observe chaotic orbits at both low and high flow rates, and the chaotic oscillations at high flow rate resulting from a cascade

of periodic-doubling bifurcation. Thus, we conclude that the flow rate k_f does play an important role in the bifurcations of the model. All the results enrich our understanding of complex oscillations in BZ reaction model.

References

- Bi, Q. S. [2010] “The mechanism of bursting phenomena in Belousov–Zhabotinsky (BZ) chemical reaction with multiple time scales,” *Sci. China Technol. Sci.* **53**, 748–760.
- Doedel, E., Champneys, A., Dercole, F., Fairgrieve, T., Kuznetsov, Yu., Oldeman, B., Paffenroth, R., Sandstede, B., Wang, X. & Zhang, C. [2007] “Auto-07p: Software for continuation and bifurcation problems in ordinary differential equations,” available via <http://cmvl.cs.concordia.ca/auto>.
- Dolzmann, K., Kaltenbach, S., Hanke, W. & Fernandes De Lima, V. M. [2007] “Biphasic optical signal of an oscillating nonstationary Belousov–Zhabotinsky bulk reaction and its similarity to some neurophysiological events,” *Int. J. Bifurcation and Chaos* **17**, 1329–1335.
- Freire, J. G., Field, R. J. & Gallas, J. A. C. [2009] “Relative abundance and structure of chaotic behavior: The nonpolynomial Belousov–Zhabotinsky reaction kinetics,” *J. Chem. Phys.* **131**, 044105-1–8.
- Györgyi, L. & Field, R. J. [1991] “Simple models of deterministic chaos in the Belousov–Zhabotinsky reaction,” *J. Phys. Chem.* **95**, 6594–6602.
- Györgyi, L., Rempe, S. L. & Field, R. J. [1991] “A novel model for the simulation of chaos in low-flow-rate CSTR experiments with the Belousov–Zhabotinsky reaction: A chemical mechanism for two-frequency oscillations,” *J. Phys. Chem.* **95**, 3159–3165.
- Györgyi, L. & Field, R. J. [1992] “A three-variable model of deterministic chaos in the Belousov–Zhabotinsky reaction,” *Nature* **355**, 808–810.
- Guo, L. Z., Guo, Y. Z., Zhao, Y. F., Billings, S. A., Coca, D. & Lang, Z. Q. [2014] “A spatial frequency domain analysis of the Belousov–Zhabotinsky reaction,” *Int. J. Bifurcation and Chaos* **24**, 1450031-1–14.
- Jing, Z. J., Wang, J. L. & Chen, L. N. [2002] “Computation of limit cycle via higher order harmonic balance approximation and its application to a 3-bus power system,” *IEEE Trans. Circuits Syst.* **49**, 1360–1369.
- Keener, J. P. & Tyson, J. J. [1986] “Spiral waves in the Belousov–Zhabotinsky reaction,” *Physica D* **21**, 307–324.
- Kuhnert, L. [1986] “A heterogeneous oscillator of the Belousov–Zhabotinsky-type in the bromate-malonic acid-cerium system induced by commercial ion-sensitive electrodes,” *React. Kinet. Catal. Lett.* **31**, 227–233.
- Li, Y. N., Chen, L., Cai, Z. S. & Zhao, X. Z. [2002a] “Study of the hyperchaos and their synchronization in the Belousov–Zhabotinsky chemical reaction,” *Acta Chimica Sinica* **60**, 1173–1178 (in Chinese).
- Li, Y. N., Chen, L., Cai, Z. S. & Zhao, X. Z. [2002b] “Chaos synchronization in the Belousov–Zhabotinsky chemical reaction by adaptive control scheme,” *Chinese J. Chem.* **20**, 753–759.
- Li, Q. S. & Zhu, R. [2004] “Mesoscopic description of chemical supercritical Hopf bifurcation,” *Int. J. Bifurcation and Chaos* **14**, 2393–2397.
- Li, M. M. [2012] “Dynamics analysis in the Belousov–Zhabotinsky reaction,” Master’s thesis, Beijing University of Chemical Technology (in Chinese).
- Li, M. M. & Chang, Y. [2012] “Complex dynamic in the Belousov–Zhabotinsky reaction,” *J. Beijing Univ. Chem. Technol.* **39**, 116–121 (in Chinese).
- Marts, B., Martinez, K. & Lin, A. L. [2004] “Front dynamics in an oscillatory bistable Belousov–Zhabotinsky chemical reaction,” *Phys. Rev. E* **70**, 056223.
- Mees, A. I. & Chua, L. O. [1979] “The Hopf bifurcation theorem and its applications to nonlinear oscillations in circuits and systems,” *IEEE Trans. Circuits Syst.* **26**, 235–254.
- Mees, A. I. [1981] *Dynamics of Feedback Systems* (Wiley, Chichester).
- Moiola, J. L., Desages, A. C. & Romagnoli, J. A. [1991] “Degenerate Hopf bifurcation via feedback system theory: Higher-order harmonic balance,” *Chem. Eng. Sci.* **46**, 1475–1490.
- Moiola, J. L. & Chen, G. R. [1993] “Computations of limit cycles via higher order harmonic balance approximation,” *IEEE Trans. Automat. Contr.* **38**, 782–790.
- Moiola, J. L. & Chen, G. R. [1996] *Hopf Bifurcation Analysis: A Frequency Domain Approach* (World Scientific, Singapore).
- Wang, J. C., Zhao, J. P., Chen, Y., Gao, Q. Y. & Wang, Y. M. [2005] “Coexistence of two bifurcation regimes in a closed ferriin-catalyzed Belousov–Zhabotinsky reaction,” *J. Phys. Chem. A* **109**, 1374–1381.
- Wiggins, S. [1990] *Introduction to Applied Nonlinear Dynamical Systems and Chaos* (Springer-Verlag, Berlin).
- Zhang, D., Györgyi, L. & Peltier, W. R. [1993] “Deterministic chaos in the Belousov–Zhabotinsky reaction: Experiments and simulations,” *Chaos* **3**, 723–745.
- Zhou, L. Q. & Yang, Q. O. [2000] “Spiral instabilities in a reaction–diffusion system,” *J. Phys. Chem.* **105**, 112–118.
- Zong, C. Y., Gao, Q. Y., Wang, Y. W., Feng, J. M., Mao, S. C. & Zhang, L. [2007] “Period-doubling and chaotic oscillations in the ferriin-catalyzed Belousov–Zhabotinsky reaction in a CSTR,” *Sci. China Series: Chem.* **50**, 205–211.